Supplementary Material

Supplementary Materials

5-Aminolevulinic acid (ALA), 2',7'-dichlorofluorescein diacetate (DCFH-DA), 1,3-Diphenylisobenzofuran (DPBF), the PPARγ antagonist GW9662 and anti-LXR antibody were purchased from Sigma-Aldrich (St Louis, MO, USA). Singlet oxygen sensor green (SOSG) was obtained from Invitrogen (MA, USA). Protoporphyrin IX (PpIX) was purchased from Macklin Inc. (Shanghai, China). Phorbol-12-myristate-13-acetate (PMA) was obtained from EMD Biosciences, Inc. (La Jolla, CA, USA). oxLDL, HDL and apoA1 were purchased from Union-Biology Co., Ltd. (Beijing, China). Total and free cellular cholesterol continuous cycle enzymatic colorimetric kits were purchased from Genmed Scientific, Inc. (Arlington, MA, USA). pHrodoTM Red SE was purchased from Molecular Probes (Carlsbad, CA, USA). X-tremeGENE siRNA Transfection Reagent and an *In Situ* Cell Death Detection Kit, POD, were purchased from Roche Applied Science (Lewes, UK). Antibodies against CD68, PPARγ, CD36, ABCA1, TGFβ and IL-10 were purchased from Abcam (Cambridge, UK). Antibodies against ABCG1, GADD153, MerTK, cytochrome c and β-actin were purchased from Santa Cruz Biotechnology, Inc. (Santa Cruz, CA, USA). Antibody against cleaved caspase 3 was purchased from Cell Signaling Technology (Beverly, MA, USA). Anti-α smooth muscle actin (α-SMA) Antibody was purchased from Boster Biological Technology (Wuhan, China). Anti-TOM20 antibody was purchased from Bioss (Beijing, China). Anti-Mouse CD11b PerCP-Cyanine5.5 was purchased from Thermo Fisher Scientific (Beverly, MA, USA). Mouse IL-10 and TGFβ ELISA kits were obtained from NeoBioscience Technology Co., Ltd. (Shenzhen, China).

Supplementary Methods

Accumulation of ALA-PpIX in Mouse Atherosclerotic Plaque
To determine time point at which ALA accumulated to the maximum in atherosclerotic plaque, apoE$^{-/-}$ mice were administered with ALA (60 mg/kg) into the caudal vein, and sacrificed at 0, 1, 2, 3, 4 and 6 h post ALA injection, respectively (n=6). Cryosections of aortic root were obtained for detecting ALA-PpIX in atherosclerotic plaques with fluorescence spectrometer (USB2000, Ocean Optics Inc., USA). Fluorescence spectra were excited by illumination of 405 nm violet light with a linewidth of 20 nm. Emission spectra from 450 to 830 nm were collected. Data were analyzed by the OriginLab OriginPro 7.0 software.

ALA-PpIX distribution analysis
In vivo, fresh-frozen sections of aortic root of apoE$^{-/-}$ mice were obtained for fluorescent detection of ALA-PpIX distribution by fluorescence microscope (Olympus, Tokyo, Japan) at 2 h following injection of ALA (60 mg/kg) into the caudal vein (n=6). Immunofluorescent staining of macrophages (anti-CD68), smooth muscle cells

(anti-α-SMA) and mitochondria (anti-TOM20) was performed to detect ALA-PpIX distribution within plaques.

Histological assay

The systemic effects of ALA-SDT were evaluated with hematoxylin and eosin (H&E) staining. 1 Day after ALA-SDT treatment, tissues of apoE$^{-/-}$ mice were collected and embedded in paraffin. Then the sectioned slices were subjected to H&E staining according to routine histopathological methods.

ROS assessment *in vivo*

The levels of ROS within atherosclerotic plaques were assessed by the ROS indicator DCFH-DA. Briefly, fresh-frozen sections of apoE$^{-/-}$ mice aortic root were obtained immediately after ALA-SDT treatment. 10 µM DCFH-DA was added to the slide and incubated at 37°C for 30 min in the dark. The nuclei were counterstained with DAPI for 10 min. The cryosections were then washed carefully three times with PBS and observed under fluorescence microscopy at once. DCF fluorescence was measured at 488 nm excitation and 525 nm emission wavelengths.

ROS assessment *in vitro*

The *in vitro* ROS generation by SDT was estimated by DCFH-DA[1], and singlet oxygen generation was estimated by SOSG[2] and DPBF[3] as described previously. Briefly, 10 µM DCFH-DA, 5 µM SOSG or 20 µM DPBF was added to water containing 0.5 mM or 1 mM PpIX respectively. The solution was exposed to ultrasound while being kept in the dark. After being exposed, the fluorescence intensity of DCF and SOSG was measured using a fluorescence microplate reader (Tecan, Switzerland; Ex/Em=488/525 nm and 504/525 nm respectively). DPBF was determined using the UV-vis spectrometer (Varian Australia Pty Ltd., Australia) by measuring absorbance at 413 nm.

The ROS generation in foam cells by ALA-SDT treatment was estimated by DCFH-DA at 0, 0.5, 1, 2, 3, 4 h after the treatment. Briefly, foam cells were stained with 10 µM DCFH-DA at 37°C for 30 min in the dark. The nuclei were counterstained with Hoechst33342 for 10 min. Then the foam cells were observed under fluorescence microscopy at once. DCF was measured at 488 nm excitation and 525 nm emission wavelengths.

Lipid analysis

Mouse serum samples were collected prior to tissue harvest. The total cholesterol level in serum was measured enzymatically using a kit from Sigma Chemical Co..

References

1.   Montesinos VN, Sleiman M, Cohn S, Litter MI, Destaillats H. Detection and quantification of reactive oxygen species (ROS) in indoor air. Talanta. 2015; 138: 20-7.

2.   Tang Q, Cui J, Tian Z, Sun J, Wang Z, Chang S, et al. Oxygen and indocyanine green loaded phase-transition nanoparticle-mediated photo-sonodynamic cytotoxic effects on rheumatoid arthritis fibroblast-like synoviocytes. International journal of nanomedicine. 2017; 12: 381.

3.   You DG, Deepagan V, Um W, Jeon S, Son S, Chang H, et al. ROS-generating TiO 2 nanoparticles for non-invasive sonodynamic therapy of cancer. Scientific reports. 2016; 6: 23200.

Supplementary Figures and Figure legends
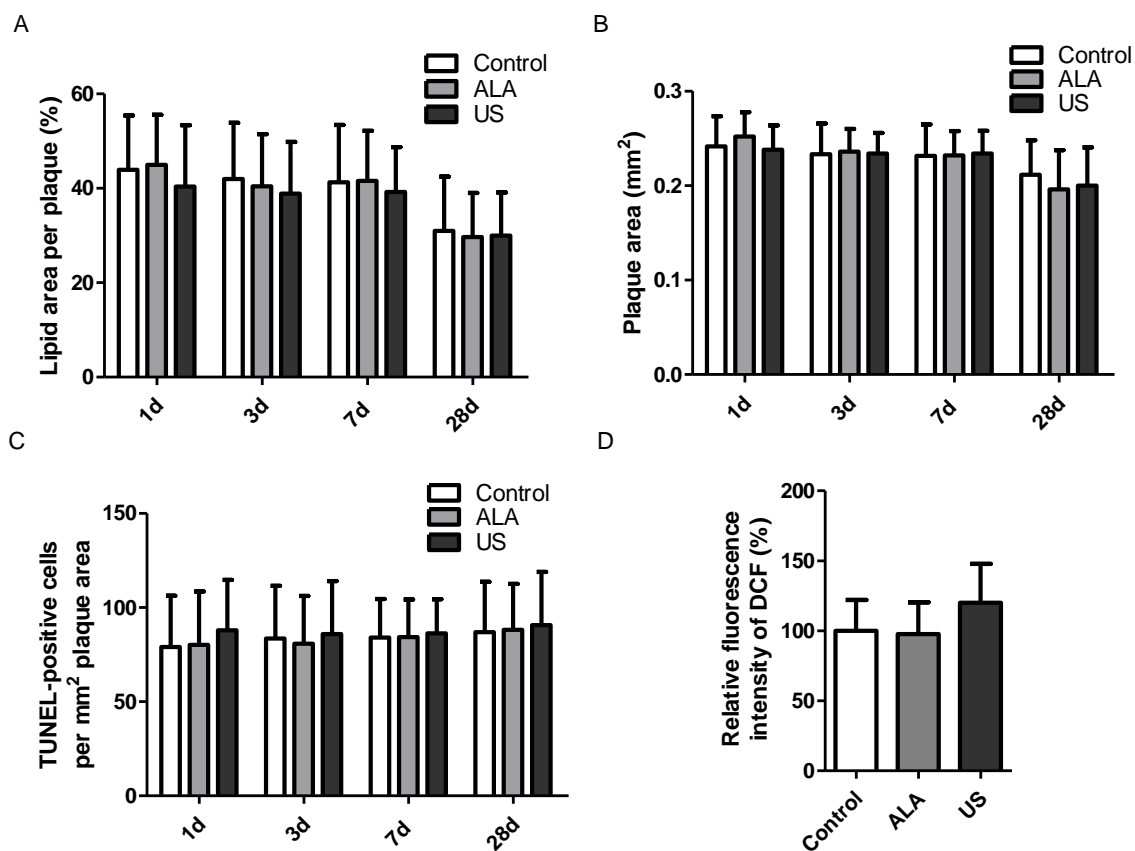
A

B

C

D

Figure S1. ALA or Ultrasound (US) treatment alone has no effect on apoE^{-/-} mice. (A-C) Quantitative analysis of lipid area per plaque (A), plaque area (B) and TUNEL-positive cells per mm^2 plaque area (C). **(D)** ROS generation in mouse atherosclerotic plaque was detected by DCFH-DA after the treatment. Levels of ROS determined by the fluorescent intensity of DCF. (n=6) Data are expressed as mean ± SD.
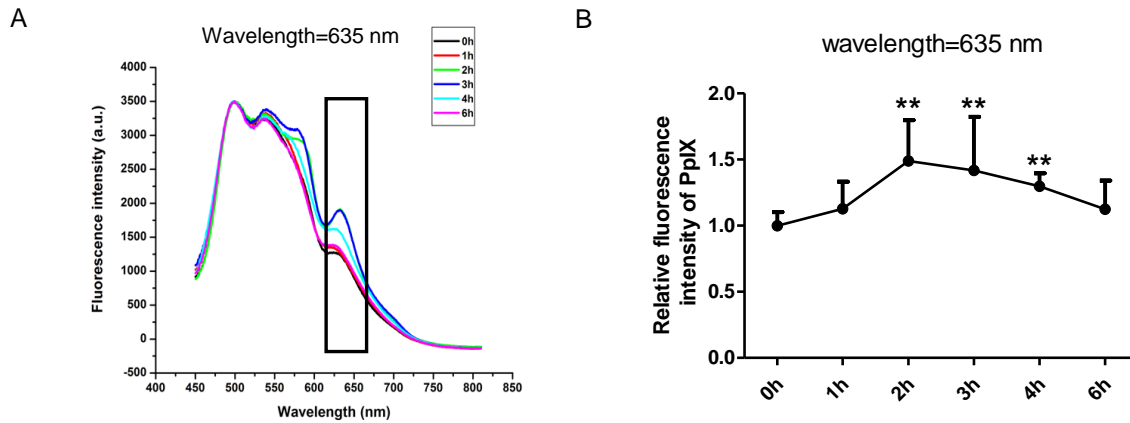
Figure S2. Accumulation of ALA-PpIX in Mouse Atherosclerotic Plaque. ApoE$^{-/-}$ mice were administered with ALA (60 mg/kg) into the caudal vein and sacrificed at 0, 1, 2, 3, 4 and 6 hours afterwards respectively. Cryosections of arteries were obtained for detecting ALA-PpIX in atherosclerotic plaque. **(A)** The typical emission spectrum of ALA-PpIX at 635 nm under excitation of 405 nm violet light was detected by fluorescence spectrometer. **(B)** The fluorescence intensity of ALA-PpIX in lesions of apoE$^{-/-}$ mouse aortic roots after intravenous ALA administration was calculated. (n=6) Data are expressed as mean ± SD; **$P<0.01$ vs. 0 h.
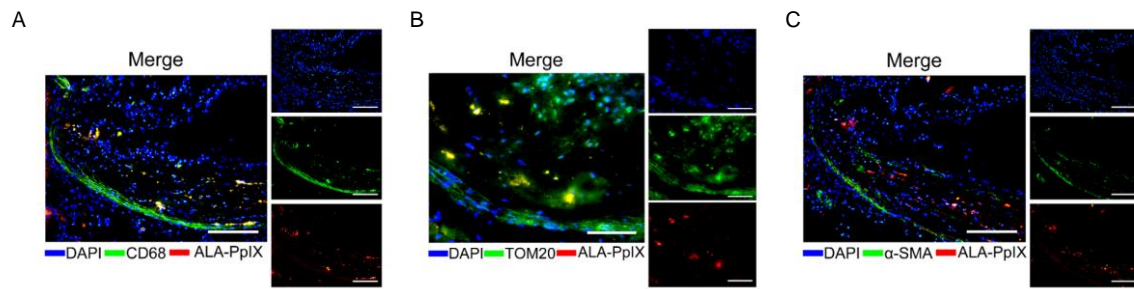
Figure S3. Distribution of ALA-PpIX *in vivo*. ApoE$^{-/-}$ mice were administered with ALA (60 mg/kg) into the caudal vein and sacrificed at 2 hour afterwards. Cryosections of aortic root were obtained for detecting the distribution of ALA-PpIX *in vivo* by fluorescence microscope (red). **(A)** Representative fluorescence micrograph of aortic root stained with macrophage marker CD68 (green) and counterstained with DAPI (blue) for nuclei. **(B)** Representative fluorescence micrograph of aortic root stained with mitochondrial marker TOM20 (green) and counterstained with DAPI (blue) for nuclei. **(C)** Representative fluorescence micrograph of aortic root stained with smooth muscle marker α-SMA (green) and counterstained with DAPI (blue) for nuclei. (n=6) Scale bar: 200 μm.
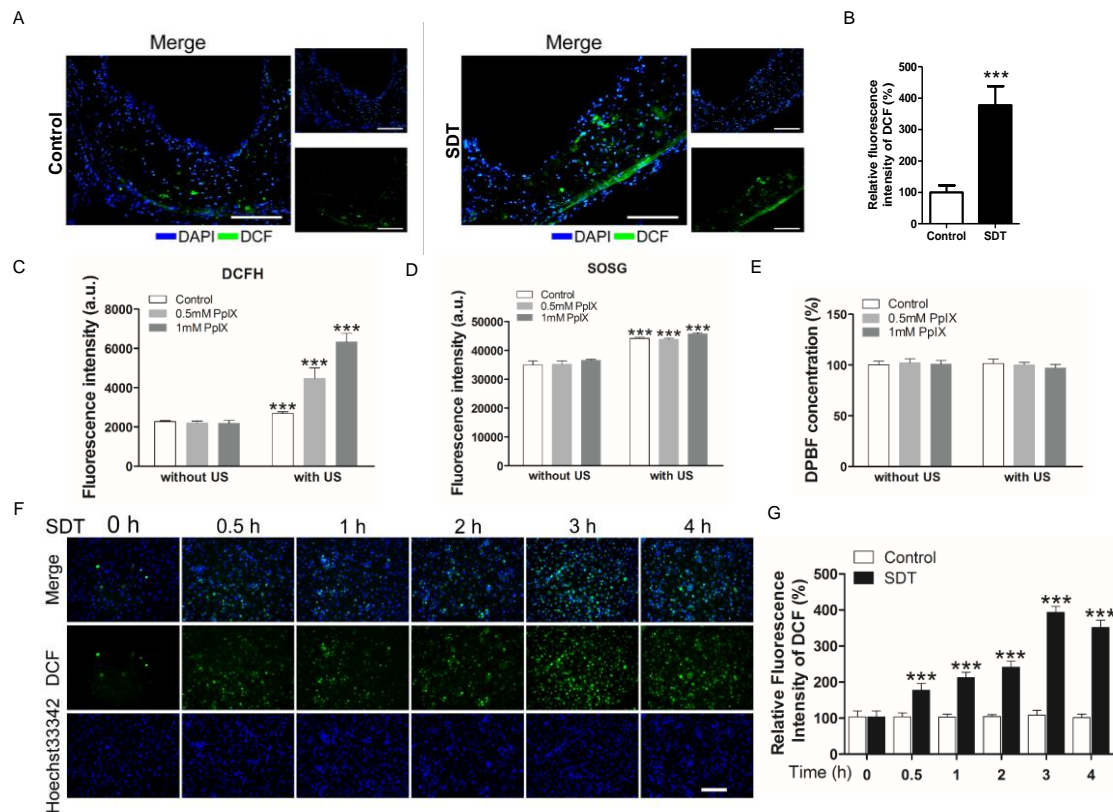
Figure S4. Effects of ALA-SDT on ROS generation *in vivo* and *in vitro*. (A, B) Effects of ALA-SDT on ROS generation in mouse atherosclerotic plaque *in vivo*. **(A)** Representative fluorescence micrographs of aortic root stained with the ROS indicator DCFH-DA (green) and counterstained with DAPI (blue) for the nuclei. Scale bar: 200 μm. **(B)** Levels of ROS determined by the fluorescent intensity of DCF in (A). (n=6) **(C-E)** Effects of ALA-SDT on ROS generation in water *in vitro*. **(C)** Levels of ROS determined by the fluorescent intensity of DCF. **(D)** Levels of singlet oxygen generation determined by the fluorescent intensity of SOSG. **(E)** Levels of singlet oxygen generation determined by the absorbance of DPBF. **(F, G)** Effects of ALA-SDT on ROS generation in foam cells *in vitro*. **(F)** Representative fluorescence micrographs of foam cells stained with DCFH-DA (green) and counterstained with Hoechst33342 (blue) for the nuclei. Scale bar: 200 μm. **(G)** Levels of ROS determined by the fluorescent intensity of DCF in (F). The assessment was performed in triplicate. Data are expressed as mean ± SD; ***$P<0.001$ vs. Control group.
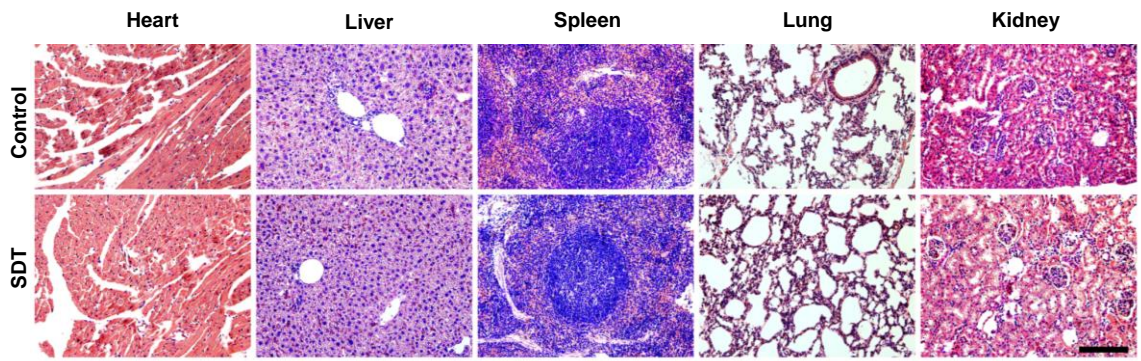
Figure S5. Systemic effect of ALA-SDT *in vivo*. Representative microphotographs of H&E staining showed that the efficacy of ALA-SDT had no significant systemic side effects in the mice model. Scale bar: 200 μm.
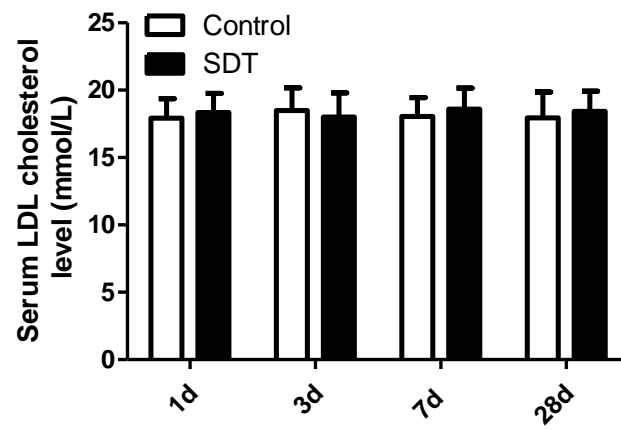
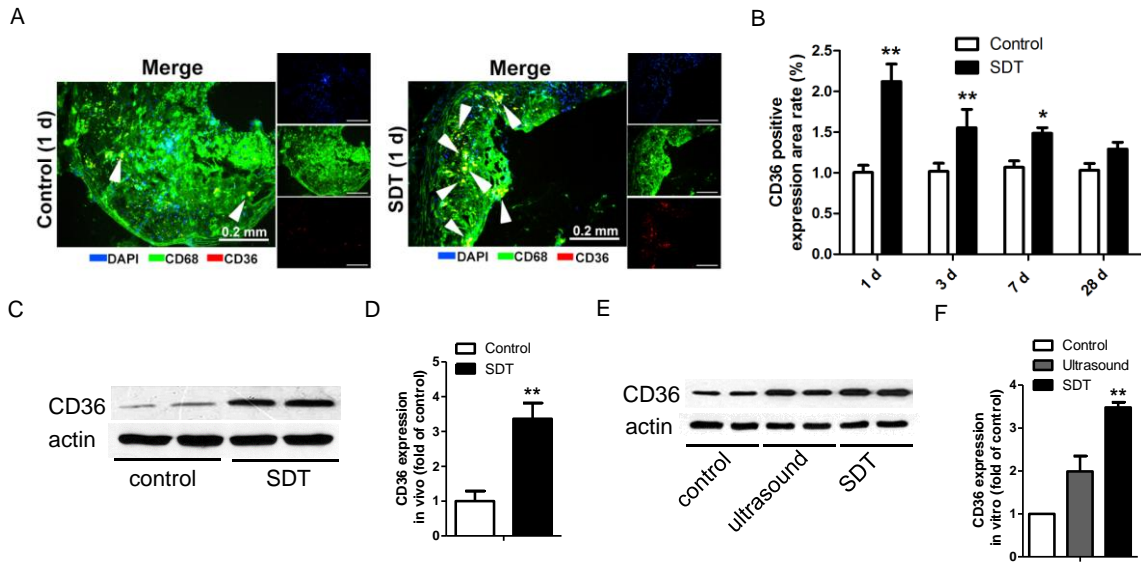**Figure S6. Serum LDL cholesterol level in apoE$^{-/-}$ mice.**

Figure S7. ALA-SDT treatment increases CD36 expression both *in vivo* and *in vitro*. (A) Representative fluorescence micrographs of aortic root double stained with CD68 and CD36 (arrows) and counterstained with DAPI for nuclei. **(B)** Quantification of positive area of CD36 in atherosclerotic lesions. (n=9) **(C)** CD36 expression in atherosclerotic lesions was detected by western blot. **(D)** Quantification of CD36 expression in (C). (n=6) **(E)** CD36 expression in phagocytes after co-incubation with supernatants of foam cells from different treatment groups was detected by western blot *in vitro*. **(F)** Quantification of CD36 expression in (E). The assessment was performed in triplicate. Data are expressed as mean ± SD; *$P<0.05$ vs. Control group, **$P<0.01$ vs. Control group.